Structure, Volume *24*

Supplemental Information

Molecular Plasticity of the Human Voltage-Dependent Anion Channel Embedded Into a Membrane

Lin Ge, Saskia Villinger, Stefania A. Mari, Karin Giller, Christian Griesinger, Stefan Becker, Daniel J. Müller, and Markus Zweckstetter

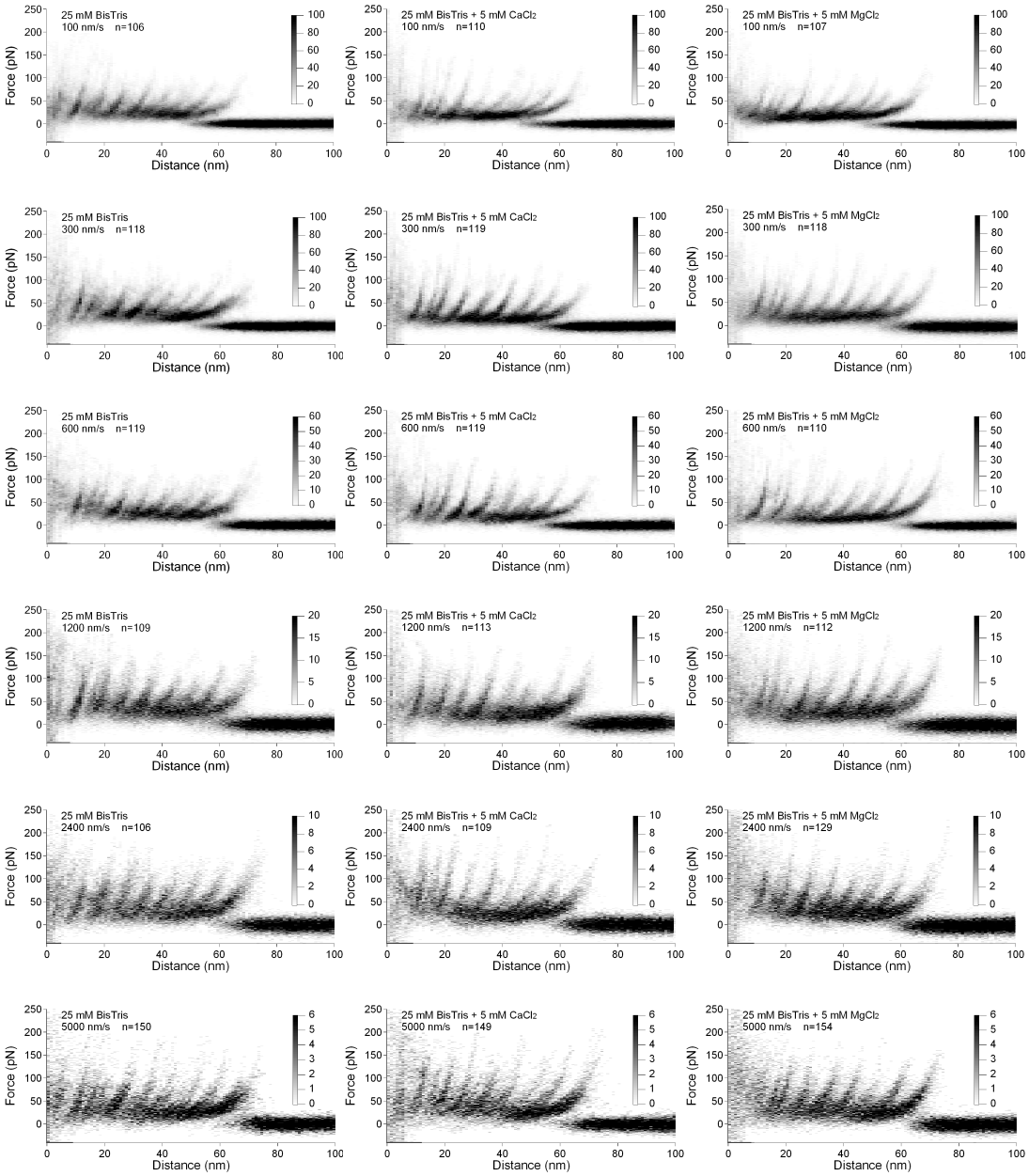

Figure S1, relates to Figure 3 and Table 1. Superimposition of FD curves recorded upon unfolding of hVDAC1 in the absence and in the presence of calcium or magnesium. Buffer conditions, pulling velocities, and number (*n*) of superimposed FD curves are indicated. Every superimposed FD curve has been recorded upon unfolding of a single hVDAC1 channel. The gray scale bar on the right allows the evaluation of events of high (black), lower (gray), and no (white) occurrence. Single-molecule force spectroscopy was recorded in buffer solution (25 mM BisTris, pH 6.8) and as indicated in the absence or in the presence of 5 mM Ca^{2+} or 5 mM Mg^{2+}.

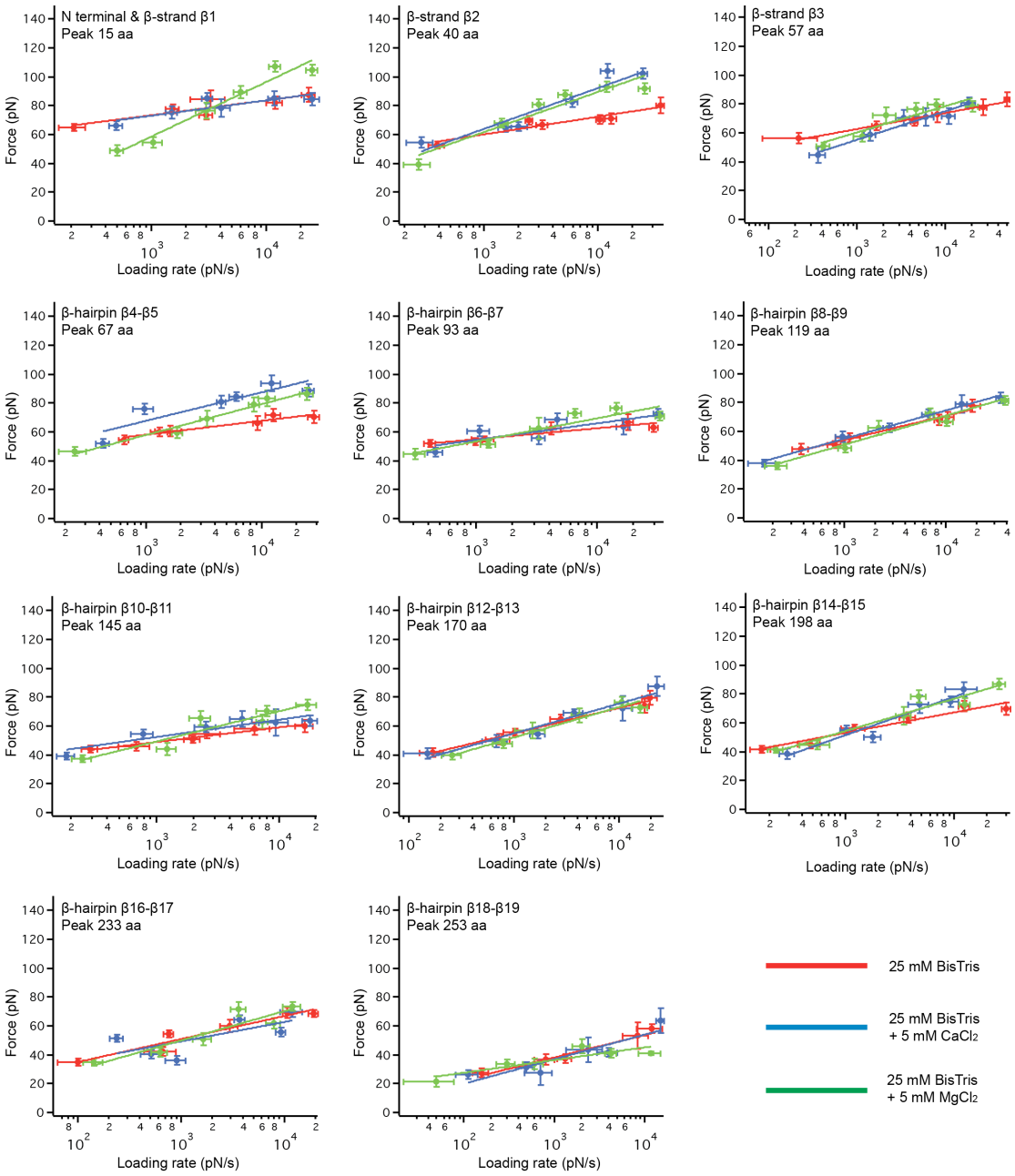

Figure S2, relates to Table 1. Dynamic single-molecule force spectroscopy (DFS) plots reveal loading rate dependent interactions stabilizing the structural segments of hVDAC1. For each stable structural segment of hVDAC1 the most probable unfolding force was determined from the raw data (**Figure S1**) and plotted against the loading rate (Experimental Procedures). The fits of the experimental data (solid lines) using Eq. 1–3 are shown for hVDAC1 unfolded in the absence of divalent ions (red), 5 mM Ca^{2+} (blue), or 5 mM Mg^{2+} (green). Values for x_u and k_0 obtained from fitting the DFS plots are given in **Table 1**. Error bars represent the standard error of most probable force and loading rate.

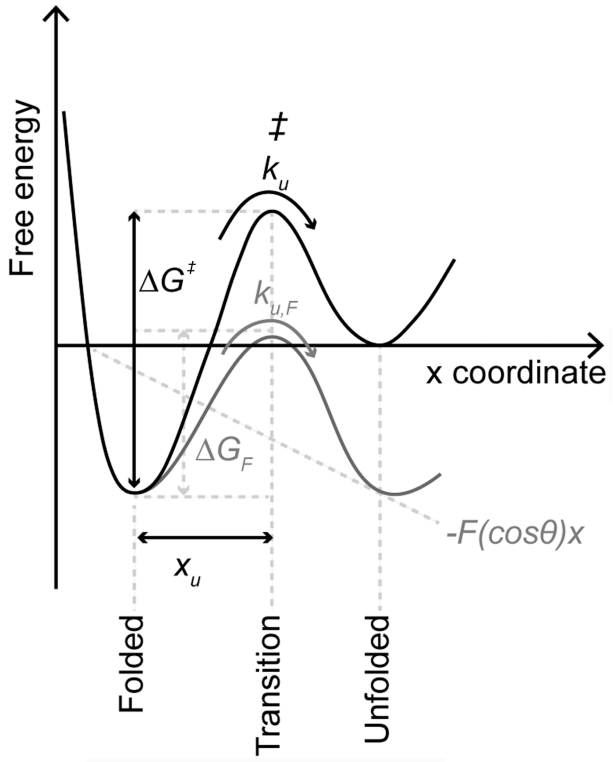

Figure S3, relates to Table 1 and Figure 5. Schematic of an energy barrier stabilizing a structural segment of hVDAC1 against unfolding. The folded state of a structural segment (e.g., for example a β-hairpin in case of hVDAC1) is separated from the unfolded state by a free energy barrier. In the absence of an externally applied force (i.e., at equilibrium) the folded structure can unfold at a certain transition rate (k_u). To unfold the structure must overcome the transition state (‡). x_u characterizes the distance from the folded state to the transition state. The height of the unfolding free energy barrier separating the folded state from the unfolded state is given by $\Delta G^{‡}$. This barrier, which is given by the free energy difference of the folded state and the transition state, therefore characterizes the activation free energy of unfolding. According to the Bell-Evans model (Bell, 1978; Evans, 1998; Evans and Ritchie, 1997), an externally applied force (F) tilts the energy landscape by the mechanical energy ($-F(\cos\theta)x$) and lowers the free energy barrier ($\Delta G^{‡}$) to ΔG_F. Lowering of the free energy barrier is described by the mechanically applied pulling direction x and the angle θ of the externally applied force (F).

Table S1, relates to Table 1. Significance tests of the parameters characterizing the energy barrier parameters x_u, k_0, and $\Delta G^{\ddagger}$ and the spring constant κ of the stable structural segments detected for hVDAC1 in different buffer solutions. Shown are *P*-values revealed from T-student tests of the parameters given in **Table 1**.

Force peak position / Structural region	Ca^{2+} *vs* control x_u	Ca^{2+} *vs* control k_u	Ca^{2+} *vs* control $\Delta G^{\ddagger}$	Ca^{2+} *vs* control κ
15 aa / N-terminus & ß1	$8.63225\ 10^{-1}$	$8.62419\ 10^{-1}$	$8.51244\ 10^{-1}$	$9.22322\ 10^{-1}$
40 aa / ß2	$3.05692\ 10^{-5}$	$2.19535\ 10^{-2}$	$2.68579\ 10^{-4}$	$5.3541\ 10^{-4}$
57 aa / ß3	$4.34067\ 10^{-7}$	$1.09213\ 10^{-2}$	$2.74325\ 10^{-7}$	$3.09731\ 10^{-4}$
67 aa / ß4-ß5	$6.22929\ 10^{-5}$	$2.69795\ 10^{-1}$	$1.4011\ 10^{-3}$	$1.53124\ 10^{-2}$
93 aa / ß6-ß7	$2.1159\ 10^{-2}$	$5.46752\ 10^{-1}$	$3.0968\ 10^{-2}$	$2.16478\ 10^{-1}$
119 aa / ß8-ß9	$1.47059\ 10^{-3}$	$7.08056\ 10^{-3}$	$1.06767\ 10^{-2}$	$4.99555\ 10^{-3}$
145 aa / ß10-ß11	$1.04417\ 10^{-1}$	$5.36127\ 10^{-1}$	$4.01567\ 10^{-1}$	$2.76425\ 10^{-1}$
170 aa / ß12-ß13	$1.51198\ 10^{-2}$	$8.58459\ 10^{-2}$	$3.10518\ 10^{-2}$	$7.42127\ 10^{-2}$
198 aa / ß14-ß15	$1.76505\ 10^{-5}$	$3.52599\ 10^{-3}$	$5.28258\ 10^{-5}$	$4.62344\ 10^{-4}$
233 aa / ß16-ß17	$4.59109\ 10^{-1}$	$4.57097\ 10^{-1}$	$5.99544\ 10^{-1}$	$4.92486\ 10^{-1}$
253 aa / ß18-ß19	$3.77248\ 10^{-1}$	$3.42859\ 10^{-1}$	$2.71483\ 10^{-1}$	$5.24156\ 10^{-1}$

Force peak at contour length (aa)	Mg^{2+} *vs* control x_u	Mg^{2+} *vs* control k_u	Mg^{2+} *vs* control $\Delta G^{\ddagger}$	Mg^{2+} *vs* control κ
15 aa / N-terminus & ß1	$4.62349\ 10^{-5}$	$2.65949\ 10^{-4}$	$6.71793\ 10^{-5}$	$6.15288\ 10^{-6}$
40 aa / ß2	$3.58609\ 10^{-5}$	$2.35747\ 10^{-2}$	$2.32124\ 10^{-4}$	$7.1667\ 10^{-4}$
57 aa / ß3	$9.48356\ 10^{-5}$	$1.94398\ 10^{-1}$	$1.35225\ 10^{-4}$	$2.83095\ 10^{-2}$
67 aa / ß4-ß5	$4.82471\ 10^{-6}$	$1.60301\ 10^{-3}$	$1.69816\ 10^{-5}$	$8.70332\ 10^{-6}$
93 aa / ß6-ß7	$1.67672\ 10^{-4}$	$1.81281\ 10^{-1}$	$3.16225\ 10^{-4}$	$7.60199\ 10^{-3}$
119 aa / ß8-ß9	$8.89912\ 10^{-3}$	$3.84503\ 10^{-2}$	$4.15668\ 10^{-3}$	$6.70167\ 10^{-2}$
145 aa / ß10-ß11	$4.37276\ 10^{-6}$	$4.88016\ 10^{-2}$	$1.79251\ 10^{-5}$	$2.63014\ 10^{-3}$
170 aa / ß12-ß13	$4.1602\ 10^{-3}$	$1.25082\ 10^{-2}$	$1.7947\ 10^{-3}$	$3.21037\ 10^{-2}$
198 aa / ß14-ß15	$2.3926\ 10^{-4}$	$2.90302\ 10^{-2}$	$1.33695\ 10^{-3}$	$4.25575\ 10^{-3}$
233 aa / ß16-ß17	$3.60765\ 10^{-2}$	$1.4135\ 10^{-1}$	$4.34655\ 10^{-2}$	$1.36833\ 10^{-1}$
253 aa / ß18-ß19	$4.43563\ 10^{-3}$	$4.46661\ 10^{-3}$	$9.94509\ 10^{-3}$	$1.51084\ 10^{-3}$

Supplemental References

Bell, G.I. (1978). Models for the specific adhesion of cells to cells. Science *200*, 618-627.

Evans, E. (1998). Energy landscapes of biomolecular adhesion and receptor anchoring at interfaces explored with dynamic force spectroscopy. Faraday Discussions *111*, 1-16.

Evans, E., and Ritchie, K. (1997). Dynamic strength of molecular adhesion bonds. Biophys J *72*, 1541-1555.